J. Cell. Mol. Med. Vol 14, No 5, 2010 pp. 1125-1134

Development of c-kit immunopositive interstitial cells of Cajal in the human stomach

Goran Radenkovic [a, *], Vojin Savic [b], Dejan Mitic [c], Srdjan Grahovac [c], Marija Bjelakovic [d], Miljan Krstic [b]

[a] Department of Histology and Embryology, Faculty of Medicine, University of Nis, Nis, Serbia
[b] Department of Pathology, Faculty of Medicine, University of Nis, Nis, Serbia
[c] Clinic of Gynaecology and Obstetrics, Nis Clinical Center, Nis, Serbia
[d] Department of Anatomy, Faculty of Medicine, University of Nis, Nis, Serbia

Received: June 4, 2008; Accepted: January 26, 2009

Abstract

Interstitial cells of Cajal (ICC) include several types of specialized cells within the musculature of the gastrointestinal tract (GIT). Some types of ICC act as pacemakers in the GIT musculature, whereas others are implicated in the modulation of enteric neurotransmission. Kit immunohistochemistry reliably identifies the location of these cells and provides information on changes in ICC distribution and density. Human stomach specimens were obtained from 7 embryos and 28 foetuses without gastrointestinal disorders. The specimens were 7–27 weeks of gestational age, and both sexes are represented in the sample. The specimens were exposed to anti-c-kit antibodies to investigate ICC differentiation. Enteric plexuses were immunohistochemically examined by using anti-neuron specific enolase and the differentiation of smooth muscle cells (SMC) was studied with anti-α smooth muscle actin and anti-desmin antibodies. By week 7, c-kit-immunopositive precursors formed a layer in the outer stomach wall around myenteric plexus elements. Between 9 and 11 weeks some of these precursors differentiated into ICC. ICC at the myenteric plexus level differentiated first, followed by those within the muscle layer: between SMC, at the circular and longitudinal layers, and within connective tissue septa enveloping muscle bundles. In the fourth month, all subtypes of c-kit-immunoreactivity ICC which are necessary for the generation of slow waves and their transfer to SMC have been developed. These results may help elucidate the origin of ICC and the aetiology and pathogenesis of stomach motility disorders in neonates and young children that are associated with absence or decreased number of these cells.

Keywords: development • interstitial cells of Cajal • pacemaker • immunohistochemistry • foetal stomach

Introduction

The term 'interstitial cells of Cajal' (ICC) has been adopted to refer to several types of cells located in the musculature of the gastrointestinal tract (GIT), morphologically and functionally intercalated between the segments of the enteric nervous system and smooth muscle cells (SMCs). Some ICC groups act as sources of spontaneous electric slow waves responsible for paced contractions of the intestinal musculature ('intestinal pacemakers'), whereas other ICC groups are involved in the modulation of enteric neurotransmission [1–4]. ICC have been found throughout the human digestive tract, including the oesophagus, stomach, small and large intestines to the inner sphincter region of the anus [5–9].

ICC express the gene product of *c-kit*, a proto-oncogene that encodes the receptor tyrosine kinase Kit [10, 11]. Labelling of Kit receptors or *c-kit* mRNA have provided efficient means of identifying ICC at the light level in a variety of preparations, including human specimens [12]. A cytokine, termed steel factor or stem cell factor (SCF), has been identified as a *c-kit* ligand [13].

Recent studies have shown that ICC are not derived from the neural crest, but rather are mesodermal in origin [14–16]. Developmental studies suggest that some ICC and SMCs have a common precursor that expresses *c-kit* [15, 17]. Kit is important in dividing the original line of mesenchymal precursors during differentiation towards ICC or SMCs, for normal postnatal development and for maintenance of the ICC phenotype [18, 19]. SCF/Kit signalling favours the development of ICC at the myenteric plexus

*Correspondence to: Goran RADENKOVIC,
Department of Histology and Embryology, Faculty of Medicine,
University of Nis, Zoran Djindjic Blv 81, 18000 Nis, Serbia.
Tel: +381 64 1523456
Fax: +381 18 238770
E-mail: radenkog@scnet.yu

doi:10.1111/j.1582-4934.2009.00725.x

Table 1 Gestational age of specimens

Gestational age (weeks)	Embryonic period		Foetal period							
	7	8	9	10	11	12	13	14–17	18–22	23–27
Number of specimens	3	4	3	4	2	3	2	5	5	4

level (ICC-MP), whereas a lack of signalling favours development of the smooth muscle phenotype [15]. Neural crest cells (NCC) enter the GIT at week 4, migrate rostrocaudally to reach the terminal hindgut by week 7, and differentiate into neurons and glia. Neurons and glia aggregate into ganglion plexus in the myenteric region [20–22]. The submucosal plexus form approximately 2–3 weeks after the myenteric plexus. Smooth muscle differentiation follow NCC colonization of the GIT within a few weeks, also mature in a rostrocaudal direction [23]. Immunohistochemical studies have shown c-kit expressing cells in the human foetal GIT: in the stomach at 9.5 weeks, in the small bowel at 9 weeks and in the colon at 10 to 12 weeks [23–26]. In all of the mentioned organs, c-kit expressing cells firstly emerge in the myenteric plexus region, but although some authors designate them ICC-MP, others think that they are 'the pool of ICC precursors'. However, some authors have identified kit^+ cells within myenteric plexus at week 12; these then move to the periphery of ganglia by week 14 [22].

ICC show different distribution patterns and morphological features depending on their anatomical locations, according to which they are classified into several subtypes [27, 28]. At least five functional subtypes of ICC exist within the tunica muscularis of the stomach: ICC-MP form a cellular network around the myenteric plexus in the space between the circular and longitudinal muscle layers; ICC of the circular muscle (ICC-CM) are located within the circular layer; ICC of the longitudinal muscle (ICC-LM) are within the longitudinal layer; ICC of the submucosa (ICC-SM) are found at the interface between the submucosal connective tissue and the innermost muscle layer and ICC of the septa (ICC-SEP) are in the connective tissue septa which surround SMC bundles of the muscle layer. ICC are more numerous in the corpus and antrum than in the fundus of the human stomach [29–35].

ICC have a central place in research examining gastrointestinal contractions and the aetiology and pathogenesis of various motility disorders. Motility disorders, which are prevalent in the stomach, are characterized by abnormal frequency or amplitude of the slow waves and may be linked to ICC abnormalities [36, 37]. Recent research has demonstrated that ICC alterations are associated with disease: infantile hypertrophic pyloric stenosis (significant decrease in the number of ICC-CM); idiopathic gastric dilation and perforation (absence or decreased numbers of ICC-CM, ICC-LM and ICC-MP); Hirschsprung's disease (decrease in number of ICC-MP); Chagas disease; pseudo-obstruction; slow transit constipation and ulcerative colitis [38–42]. Histopathological studies on GI stromal tumours showed that they were immunopositive for the c-kit protein [43].

Investigation of immature ICC morphology, timing of appearance and organization during differentiation may help in interpreting the significance of abnormalities in ICC distribution, density and morphology at birth and during early childhood. Such research may also aid in understanding the pathophysiology of motile disorders of the stomach in neonates and young children.

The aim of the present study was to investigate the timing of appearance and distribution of ICC populations in the human stomach, in parallel with differentiation of nerve structures and SMCs. The specimens were exposed to anti-c-kit antibodies, and enteric plexuses were immunohistochemically examined by using anti-neuron specific enolase (NSE). SMC differentiation was studied immunohistochemically with anti-α smooth muscle actin (αSMA) and anti-desmin (Des) antibodies.

Materials and methods

The study material consisted of 7 human embryos and 28 human foetuses, 7–27 weeks of gestational age (Table 1). The specimens were obtained after legal abortions and premature births due to pre-partial deaths, according to the principles of the Ethical Committee. Both sexes are represented in the sample, and no specimens had gastrointestinal disorders. Gestational ages were estimated by anatomical criteria according to the Carnegie Staging system and the crown rump length, head circumference and foot length.

Each embryo and foetal stomach specimen was fixed in 10% neutral formalin and paraffin embedded. Routine histopathological examination of haematoxylin- and eosin-stained sections confirmed that stomach wall morphology was normal in all cases, although the mucosa showed autolytic alterations in several patients. The study was approved by the ethics committee of the Faculty of Medicine of University of Nis.

Consecutive 4-μm sections of foetal stomach cardias, fundus, corpus and antrum were collected and immunolabelled. Embryos were processed completely, sequentially sectioned at 4 μm and stained. Immunohistochemical analysis was performed with the detection Kit-Polymer. The sections were deparaffined in xylene, dehydrated with a descending series of alcohol rinses (less than 1 min. each) and then rehydrated in distilled water. The endogenous peroxydase was blocked with 3% H_2O_2 for 10 min. at room temperature. This was followed by incubation with the primary antibodies for 60 min. at room temperature, rinsing in a phosphate buffered solution (0.1 M PBS, pH 7.4). The primary antibodies were dissolved in Dako (Glostrup, Denmark) antibody diluent (Cat. No. S0809) (Table 2). The sections were incubated with streptavidin horseradish peroxidase conjugate for 30 min. at room temperature. The complex was visualized with DAKO Liquid DAB + Substrate/Chromogen System (Code No. K3468). All immunolabelled sections were counterstained by Mayer's haematoxylin. Immunoreactivity (IR) was absent in negative controls in which the primary antibody was omitted.

The primary antibodies used, and their respective dilutions, are listed in Table 2.

Table 2 Antibodies

Antigen	Clone	Supplier	Dilution
C-kit	CD-117	Dako	1 : 300
α-SMA	1-A4	Dako	1 : 100
NSE	BBS/NS VI-H14	Dako	1 : 100
Desmin	DE-R-11	Dako	1 : 100

Results

C-kit immunoreactivity

Embryonic period: 7 to 8 weeks

In this period of development, c-kit-IR was observed in the form of a wide belt of cells situated at the level of the myenteric plexus (Fig. 1A–C). Within the belt of c-kit-IR cells are clearly delineated groups of c-kit$^-$ cells, surrounded by, but not interspersed with, c-kit-IR cells (Fig. 1A and B). The described groups of c-kit-IR$^-$ cells are NSE-IR, confirming that they represent the inception of the myenteric plexus ganglia.

The belt of c-kit-IR cells is present throughout the stomach circumference, except in the fundus, where it is very thin or absent (Fig. 1C). C-kit-IR cells are irregular, with large oval or round nuclei. They have small bodies with few interconnecting thin cytoplasmic processes (Fig. 1B, E and F).

Foetal period: 9 to 27 weeks

At 9–10 weeks, the c-kit-IR cells are clearly located at the myenteric plexus level and c-kit-IR cells are not present within the circular muscle layer (Fig. 1D). They are densely packed and encircle small groups of c-kit-IR$^-$ cells in a manner similar to that described for the embryonic period of development.

At 11–12 weeks, numerous c-kit-IR cells are present at the myenteric plexus level (Fig. 1G, H and I). These cells are pleomorphic, but their shape seems to be different from the cells described for 7–8 weeks. Most have ovoid or triangular cell body with three or four processes by which they connect to each other, forming three-dimensional networks between muscle layers (Fig. 1G and I). ICC processes commonly branch further into secondary processes, which are also c-kit-IR (Fig. 1G and H). Some c-kit-IR cells completely encircle the myenteric plexus ganglia, but neither these cells nor their processes are present inside the ganglia (Fig. 1K). Cells which encircle the ganglia are most commonly spindle shaped, with two cellular extensions keeping them in contact with each other to form an envelope around the ganglion. All of these cells are designated ICC-MP. In this period of development, SMC can be clearly recognized, forming the circular muscle layer. C-kit-IR cells are present between these cells; they are elongated and spindle-like, with two processes each originating from opposite ends (Fig. 1L). These cells correspond to ICC-CM. They are parallel to the longitudinal axis of the adjacent SMC. ICC-CM have a very similar shape and size or slightly smaller than the adjacent SMC (Figs 1L, 2D and E). They are markedly more numerous in the outer parts of the muscle layer, near the myenteric plexus, and are rare or absent in the regions near the submucous border. In addition to ICC, we also found a large number of c-kit-IR mast cells, but they are easily distinguished from ICC on the basis of their shape and granular content (Fig. 1J).

In the fourth month of development, c-kit-IR cells are numerous throughout the circular muscle layer. They are present in the muscle bundles adjacent to the myenteric plexus and also in those situated at the submucosal border. Rarely, c-kit-IR cells are located within the poorly developed longitudinal muscle layer and can be designated as ICC-LM. These cells are spindle shaped, with two extensions each on opposite ends, orientated parallel to the major axis of SMC of the longitudinal layer. Their shape and size closely resemble the above-described ICC-CM. In this period, SMC of the circular layer are grouped into muscle bundles enveloped in thin septa made of connective tissue. C-kit-IR ICC are present inside the septa (Fig. 2A–C), most commonly spindle shaped, less frequently dendritic. They are often very elongated (Fig. 2B and C), much longer than the above-described cells, and correspond to ICC-SEP. Most ICC-SEP are perpendicular to the direction of the muscle bundles they envelop.

In the fourth and fifth months of development, differences were observed in the distribution of particular ICC types in the cardias, fundus, corpus and antrum of the stomach. In the cardias ICC-MP are absent, but ICC-CM, ICC-LM and ICC-SEP are present (Fig. 2F). In the fundus ICC-MP are absent. In the corpus ICC-MP are conspicuously present around the ganglion and between muscle layers, and ICC-CM, ICC-LM and ICC-SEP are present (Fig. 2G). ICC-MP, ICC-CM, ICC-SEP and ICC-LM are present in the antrum. ICC-CM appear to be interconnected into long rows, extending parallel to the longitudinal axis of the muscle bundles. Some of these cells possess branches which connect them to cells in neighbouring parallel rows (Fig. 2H).

Interestingly, c-kit-IR cells were found around the blood vessels in the circular muscle layer of the stomach. These cells are elongated, spindle-shaped and placed with their longitudinal axis parallel to the longitudinal axis of the blood vessel (Fig. 2I and J). They are frequently interconnected into long rows extending along the blood vessel walls (Fig. 2I).

In the sixth and seventh months of development all of the above-described c-kit-IR ICC are distributed as in previous developmental stages. ICC are most commonly bipolar, spindle shaped, with a pair of long cytoplasmic processes each on opposite ends (Fig. 3A). They appear to be linearly interconnected into long rows of cells (Fig. 3B). Sometimes bipolar ICC have branches (Figs 2H and 3C). Spindle-shaped ICC with a single long cytoplasmic process are also present, but we cannot tell with certainty if these are unipolar cells or are merely the consequence of sectioning (Fig. 3D). ICC with irregular shapes and multiple processes are also numerous and branching, interconnected into three-dimensional networks.

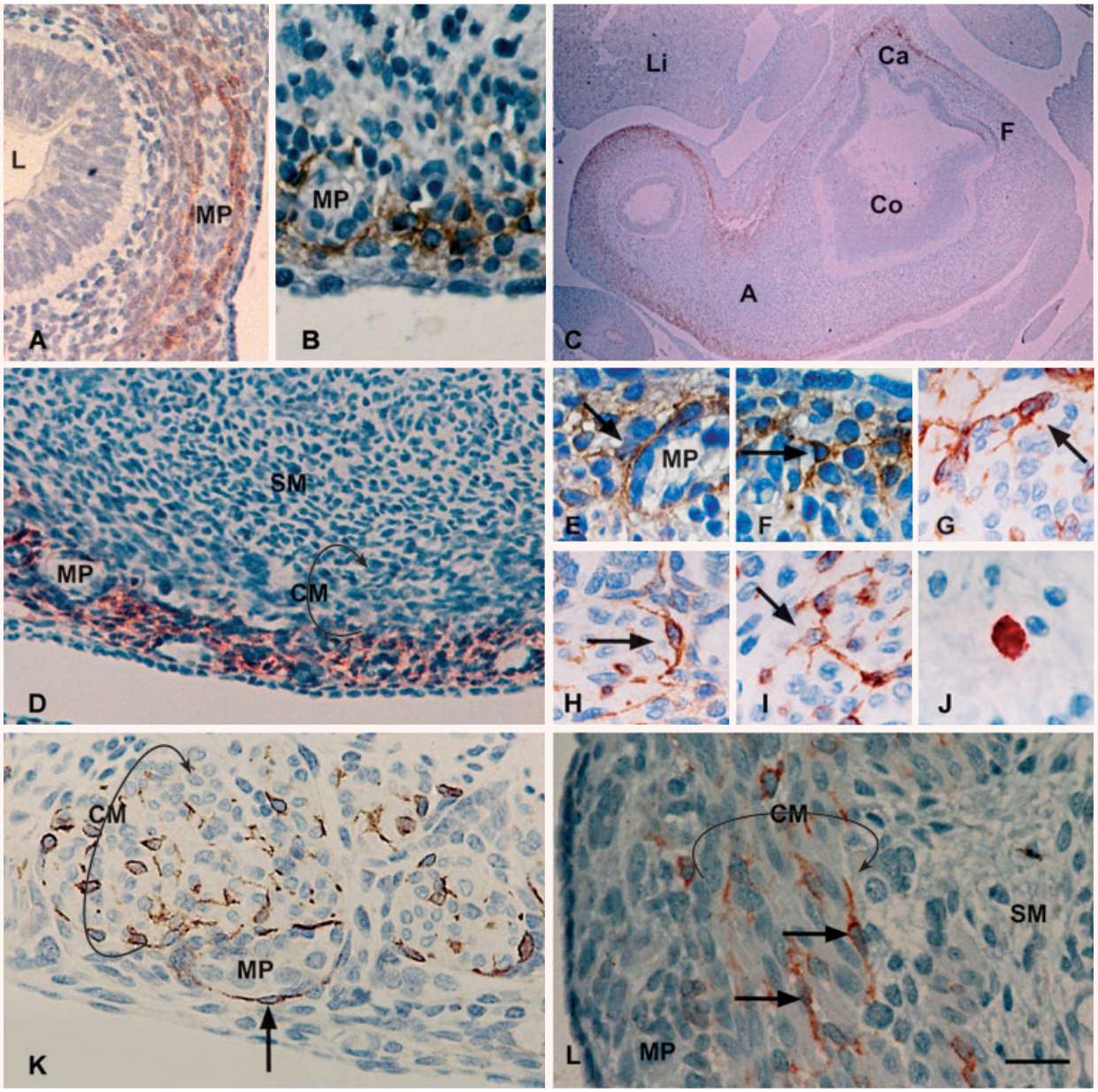

Fig. 1 c-kit immunohistochemistry. (**A**–**L**) Embryos and foetuses aged 7–14 weeks. (**A**) 7 weeks, antrum. C-kit-IR cells located in the external portion of the stomach wall, on both sides of a group of myenteric plexus elements. These cells can be considered ICC precursors. (**B**) 8 weeks, corpus. C-kit immunopositive cells are grouped at the myenteric plexus, enveloping a ganglion. These cells have small triangular body with three or more thin processes. (**C**) 8 weeks. The belt of c-kit-IR cells is present throughout the stomach circumference, except in the fundus, where it is very thin or absent. (**D**) 9 weeks, antrum. C-kit immunopositive cells are located external to the grouped myoblasts of the circular layer. (**E**) 8 weeks, corpus. C-kit-IR cell (arrow) with at least three processes. (F) 8 weeks, corpus. C-kit-IR cell (arrow) with at least three processes. (**G**) 11 weeks. An ICC-MP with three processes (arrow), one of which bifurcates. (**H**) 11 weeks, corpus. One spindle-shaped ICC-MP (arrow) with two primary processes that branch further into secondary processes. (**I**) 11 weeks, corpus. Four highly ramified ICC-MP, one of which has at least four processes (arrow). (**J**) 14 weeks, corpus. In the submucosa, isolated round c-kit-IR mast cell is seen. (**K**) 11 weeks, corpus. The arrow indicates ICC closely apposed around a ganglion. These cells can be considered ICC-MP. (**L**) 12 weeks, antrum. Two spindle-shaped ICC-CM (arrows) within the circular muscle layer. CM, circular muscle layer; MP, myenteric plexus; SM, submucosa; L, lumen; Li, liver; Ca, cardias; F, fundus; Co, corpus; A, antrum. Bar: **A**, **D** = 50 μm; **B**, **K**, **L** = 25 μm; C = 250 μm; **E**–**J** = 20 μm.

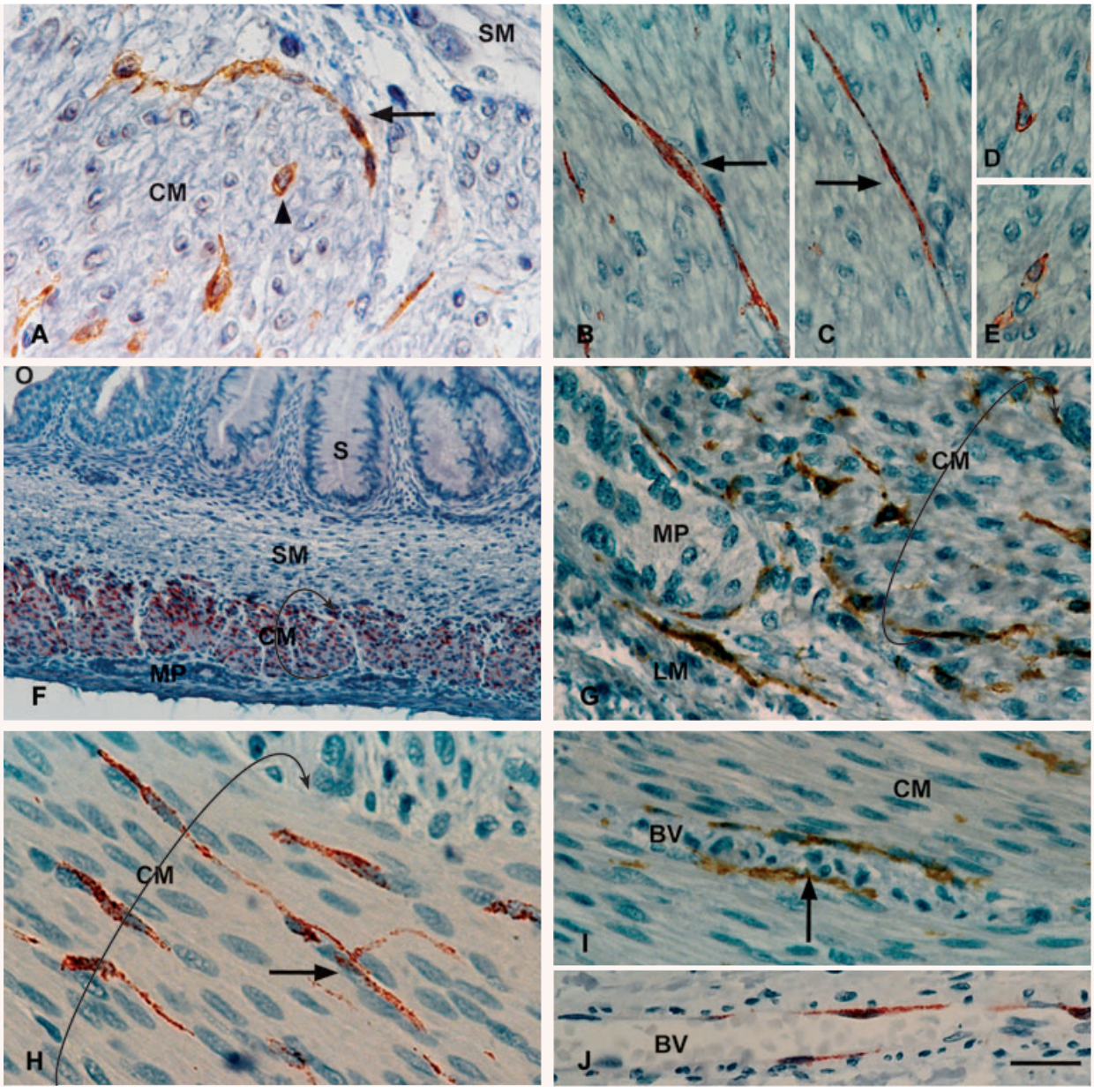

Fig. 2 c-kit immunohistochemistry. (**A**–**J**) Foetuses aged 15–27 weeks. (**A**) 21 weeks, corpus. Three ICC are interconnected (arrow) within a connective septa that envelops a bundle of smooth muscle cells. These cells can be considered ICC-SEP. The arrowhead indicates ICC-CM. (**B**, **C**) 20 weeks, corpus. Two spindle-shaped ICC-SEP (arrows) are perpendicular to the direction of the muscle bundles they envelop. These cells have two long processes starting at the opposite poles of the cell. (**D**, **E**) 20 weeks, corpus. Cross-section of two ICC-CM within muscle bundles. (**F**) 15 weeks, cardias. ICC-CM are numerous within the circular muscle layer, but there are no ICC-MP at the myenteric plexus level. (**G**) 20 weeks, corpus. ICC-MP, ICC-CM, ICC-SEP and ICC-LM are present. (**H**) 20 weeks, antrum. ICC-CM are interconnected and orientated parallel to the long axis of smooth muscle cells. An ICC-CM with two long processes, one of which bifurcates (arrow). (**I**) 19 weeks, antrum. c-kit-IR cells are present around the blood vessels. These cells are elongated, spindle-shaped and placed with their longitudinal axis parallel to the longitudinal axis of the blood vessel. (**J**) 27 weeks, corpus. Three spindle-shaped c-kit-IR cells are present around or within the blood vessel wall. O, oesophagus; S, stomach; CM, circular muscle layer; LM, longitudinal muscle layer; MP, myenteric plexus; SM, submucosa; L, lumen; BV, blood vessel. Bar: **A**–**E** = 20 μm; **F** = 100 μm; **G**–**I** = 25 μm; **J** = 35 μm.

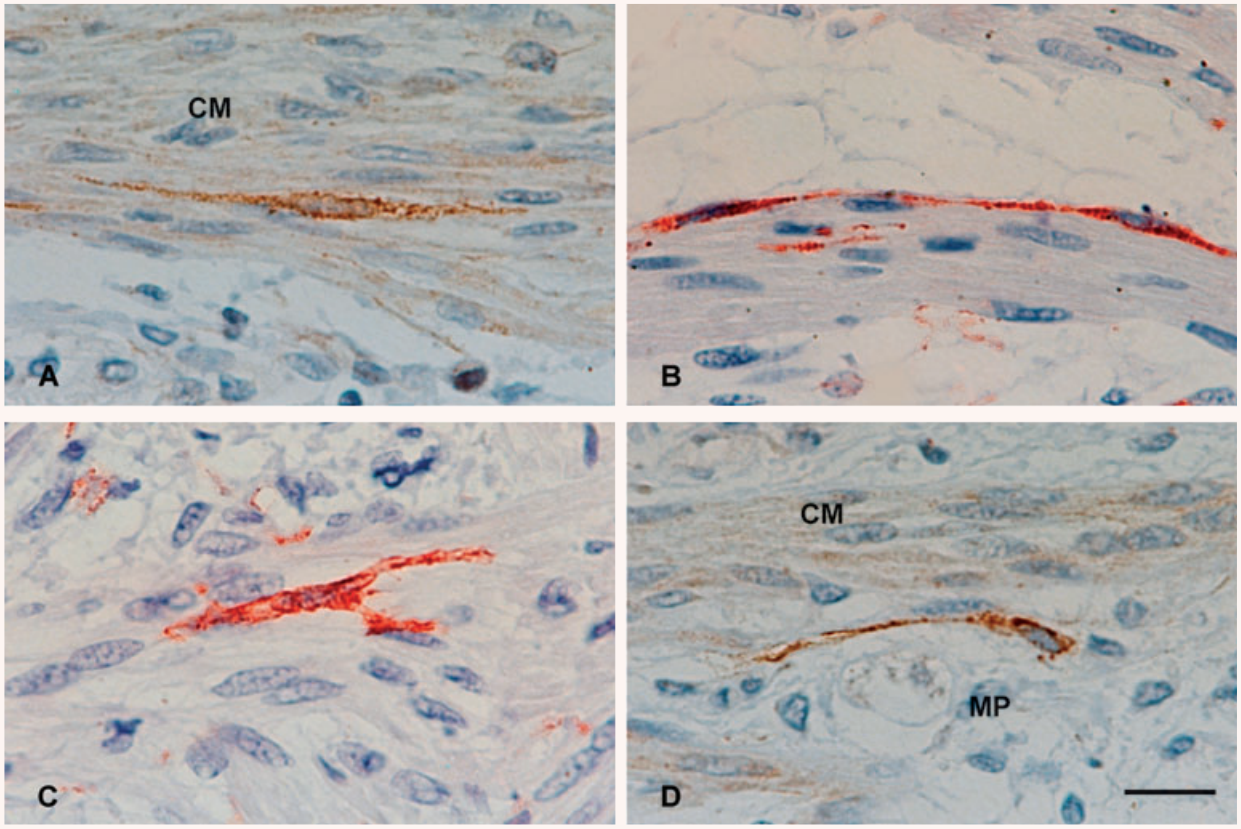

Fig. 3 c-kit immunohistochemistry. (**A**–**D**) Foetuses aged 23–25 weeks. (**A**) 23 weeks, corpus. One bipolar ICC, within the bundle of smooth muscle cells, has spindle-shaped body with two processes starting at the opposite poles of the cell. (**B**) 25 weeks, antrum. Two interconnected bipolar ICC, located on the border of bundle of smooth muscle cells. (**C**) 25 weeks, antrum. One multipolar ICC, within the bundle of smooth muscle cells, has an elongated body with four processes. (**D**) 23 weeks, corpus. One unipolar ICC, at the myenteric plexus level, has a small body with one long process. CM, circular muscle layer; MP, myenteric plexus. Bar: **A**–**D** = 20 μm.

Nerve structures and neuron specific enolase immunoreactivity

Only myenteric plexus elements were present in the embryos aged 7 weeks, and they were faintly labelled. At 8 weeks the myenteric plexus was intensely labelled (Fig. 4A). The submucous plexus was absent in the embryonic period, but it was faintly labelled in foetuses aged 9 weeks. Both the myenteric and the submucous plexuses, are present and intensely labelled in foetuses aged 12 weeks (Fig. 4B). In the older patients, nerve structures are intensely labelled and clearly visualized.

α-smooth muscle actin immunoreactivity and desmin immunoreactivity in smooth muscle layers

At the end of the embryonic period of development (7–8 weeks), αSMA-IR is present in the stomach wall in the form of a wide belt of cells (Fig. 4C). This belt incorporates the cells which will form the circular muscle layer, cells in the region of the myenteric plexus (around the myenteric ganglia) and cells external to ganglia. At weeks 11 and 12, αSMA-IR is present in the circular and longitudinal layers, although the longitudinal layer is extremely thin (Fig. 4D). In this period, the cells in the myenteric plexus region and around myenteric ganglia do not express αSMA-IR. By 15–27 weeks, the muscle layers are intensely αSMA-IR.

In the embryos aged 7–8 weeks, Des-IR is very faint and present in the form of a thin row of cells which will form the circular layer. Des-IR is not present in the myenteric plexus region (in the cells around ganglia), nor in the cells external to this region. At 9–10 weeks, Des-IR is present in the whole of the circular muscle layer, but not in the region of myenteric plexus or in the portion external to this region (Fig. 4E). At 11–12 weeks, Des-IR is intense in both circular and longitudinal muscle layers, although the longitudinal layer is very thin (Fig. 4F). By 15–27 weeks the muscle layers are intensely Des-IR.

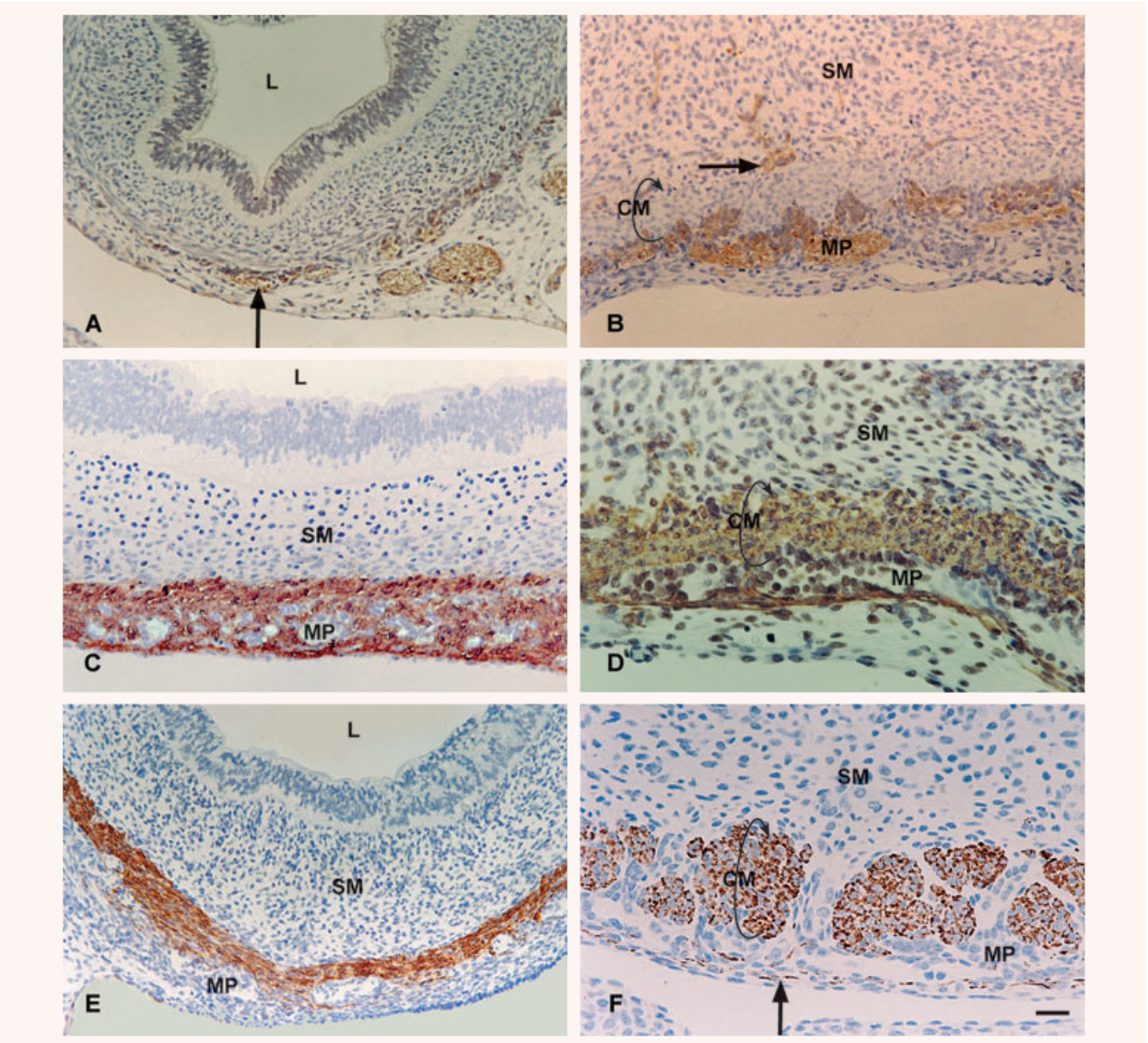

Fig. 4 Neuron-specific enolase (NSE-IR), α-smooth muscle actin (α-SMA-IR) and desmin (Des-IR) immunohistochemistry. (**A**, **B**) NSE-IR; (**C**, **D**) α-SMA-IR; (**E**, **F**) DES-IR. (**A**) 8-week-old embryo, corpus. The myenteric plexus elements are present (arrow). (**B**) 11-week-old foetus, corpus. Both the myenteric and submucous plexuses (arrow) are present. (**C**) 8-week-old embryo, antrum. α-SMA-IR is present in the form of a wide belt of cells that incorporates the cells that would form the circular muscle layer, cells in the region of the myenteric plexus (around the myenteric ganglia) and cells external to this region. (**D**) 11-week-old foetus, corpus. Both the circular and the longitudinal muscle layers are α-SMA-IR. (**E**) 10-week-old foetus, antrum. DES-IR is intense in the thin circular muscle layer. (**F**) 11-week-old foetus, corpus. Both the circular and the longitudinal muscle layers are DES-IR. The longitudinal muscle layer is very thin (arrow). CM, circular muscle layer; LM, longitudinal muscle layer; MP, myenteric plexus; SM, submucosa; L, lumen. Bar: **A**, **B**, **C**, **E** = 50 μm; **D**, **F** = 25 μm.

Discussion

The results of this investigation indicate that c-kit-IR cells are present in the human stomach wall at the end of embryonic period of development (seventh and eighth weeks). This group of cells is designated as a 'pool of ICC precursors'. The finding that these cells firstly emerge at the myenteric plexus level is in agreement with the previous studies [23–26]. However, what is important is that c-kit-IR cells are present at the myenteric

plexus level in the cardias at the end of embryonal and the beginning of foetal period. From the fourth month of development onwards, c-kit-IR ICC are present in the cardias within muscle layers, but not at the myenteric plexus level. ICC-MP are not present in the cardias of adults either [27, 34]. This finding suggests that some of the cells present in the myenteric plexus are 'responsible' for ICC differentiation, representing probably the source of SCF.

Experimental data suggest that a 'pool of ICC precursors' represent common precursors of ICC and SMC [15, 17, 19, 44–46]. There is disagreement on whether these precursors will generate only SMC of the longitudinal layer in addition to ICC, or whether they generate circular muscle cells as well. Our results demonstrate that at the end of embryonic period c-kit-IR cells are located in the external portion of the stomach wall, external to the grouped myoblasts, which are directed towards and differentiate into SMC of the circular layer. These two groups of cells are clearly separated, and c-kit-IR cells are not present within the cells that form the circular muscle layer until the middle of the third developmental month. This finding supports the theory that the circular muscle layer develops independently from c-kit-IR precursors. This does not, however, exclude the possibility that the cells of the longitudinal layer develop from precursors in common with ICC.

The differences between αSMA-IR and Des-IR expression are also important. Our results show that at the end of the embryonic period of development c-kit-IR precursors and myoblasts from the circular layer both express αSMA-IR, but that only the latter are also Des-IR, whereas c-kit-IR precursors remain Des^{-}. This finding also supports the hypothesis that the circular muscle layer develops independently from c-kit-IR precursors.

There are no previously reported data indicating the timing of ICC development from a common precursor in relation to SMC development in the human stomach [16–19, 44]. Our results indicate that the separation occurs in the beginning of the foetal period of development, at 9–11 weeks. Around week 11, the 'pool of ICC precursors' is no longer present in the myenteric plexus region and external to this region; only smaller groups or individual c-kit-IR cells can be spotted around the myenteric plexus elements, and may be designated ICC-MP. At the same time, c-kit-IR cells corresponding to ICC are present among the SMC. These can be identified as ICC-IM by their shape and location, and may be designated ICC-CM. Kenny described c-kit-IR in the longitudinal muscle layer in the human stomach at 9.5 weeks' gestation. At 12 weeks' gestation this c-kit-IR disappeared [24]. There is the question whether c-kit-IR cells, present at 9.5 weeks at the longitudinal muscle layer, belong to the 'pool of ICC precursors' which later, between 9 and 11 weeks, cease to express *c-kit* and differentiate into SMC of the longitudinal layer. Furthermore, in the 10th and 11th weeks, differentiation of SMC of the longitudinal layer occurs, resulting in cells that are αSMA-IR and Des-IR. Before this period, Des-IR was present only in the circular muscle layer.

According to some authors [22], the longitudinal and circular muscle layers appear at the same time in the human GIT. However, we have found that, in the stomach, the longitudinal muscle layer appears after the circular muscle layer. Such delayed maturation of the longitudinal muscle layer has been reported in the human foetal gut [23].

Table 3 Time course of cell type appearance

Cell types	Gestational age			
	7–9 weeks	11 weeks	13 weeks	15–27 weeks
ICC precursors	Present			
ICC-MP		Present	Present	Present
ICC-CM		Present	Present	Present
ICC-LM			Present	Present
ICC-SEP				Present

In the human GIT, the submucous plexus formed approximately 2–3 weeks after the myenteric plexus, arising from cells which migrated centripetally through the circular muscle layer from myenteric region [22, 23]. Our results show that the submucous plexus develops 2 weeks later than the myenteric plexus, in the human stomach.

Some authors [22] have identified c-kit-IR precursors within ganglia of myenteric plexus of the human foetal gut. The results of this study clearly demonstrate that at the time of occurrence of c-kit-IR cells, there are small groups of $c\text{-}kit^{-}$ cells, clearly delineated, that represent the ganglia of the myenteric plexus. C-kit-IR cells (precursors and ICC) and their processes have not been observed inside the ganglia of myenteric plexus. ICC maintain this type of distribution throughout the foetal period of development. Similar reports of ICC surrounding myenteric ganglia have been described in the human foetal small bowel [23–26].

The time of emerging of certain ICC subtypes was shown in Table 3. An identical sequence of appearance for certain ICC subtypes was described in the human intestine, but in later phases of development [23–26]. In the middle of the third month of development, ICC develop first in the myenteric plexus region (ICC-MP) *via* the differentiation of c-kit-IR precursors. These cells correspond to ICC-MP in the adult human stomach [27–29]. C-kit-IR ICC differentiate within the circular muscle layer before those located within the longitudinal muscle layer. These cells correspond to adult ICC-CM and ICC-LM [30, 34]. A final c-kit-IR ICC type appears within the connective tissue septa, which envelop the muscle bundles. This cell type has been described in adults [33], and may be designated ICC-SEP.

In a large number of samples c-kit-IR ICC were observed around the blood vessels which penetrate the circular muscle layer. However, we cannot tell with certainty whether these cells lie around the blood vessel or participate in the structure of the blood vessel wall, taking into account the fact that c-kit-IR cells have been found in the blood vessel walls in other organs [47, 48].

An important result of this study is the establishment of ICC-MP, ICC-SEP and ICC-IM presence in the human stomach wall in

the fourth month of development. ICC-MP function as electrical pacemakers, generating slow waves that control the frequency of phasic contractions of the muscle layers [10, 11]. ICC-SEP serve much like the Purkinje fibres in the heart, conveying and coordinating the spread of pacemaker activity deep into and between muscle bundles [32]. ICC-IM have two primary functions in the stomach. They are essential for a functional cholinergic excitatory and nitrergic inhibitory motor innervation of the smooth muscle [49–51]. Hence, we may conclude that in as early as the fourth month all subtypes of c-kit-IR ICC have been developed for the generation of electric impulses, as well as the basis for their transmission to the SMC.

Acknowledgements

We thank Mile Randjelovic for his technical assistance. We also thank Milkica Tosic Djordjevic for her precious help in immunohistochemical procedures.

References

1. **Thuneberg L.** Interstitial cells of Cajal: intestinal pacemaker cells? *Adv Anat Embryol Cell Biol*. 1982; 71: 1–130.
2. **Sanders KM.** A case for interstitial cells of Cajal as pacemakers and mediators of neurotransmission in the gastrointestinal tract. *Gastroenterology*. 1996; 111: 492–515.
3. **Ward SM.** Interstitial cells of Cajal in enteric neurotransmission. *Gut*. 2000; 47: 40–3.
4. **Ward SM, Sanders KM.** Physiology and pathophysiology of the interstitial cells of Cajal: from bench to bedside. I. Functional development and plasticity of interstitial cells of Cajal networks. *Am J Physiol Gastrointest Liver Physiol*. 2001; 281: G602–11.
5. **Faussone-Pellegrini MS, Cortesini C.** Ultrastructural features and localization of the interstitial cells of Cajal in the smooth muscle coat of human esophagus. *J Submicrosc Cytol*. 1985; 17: 187–97.
6. **Romert P, Mikkelsen HB.** C-kit immunoreactive cells of Cajal in the human small and large intestine. *Histochem Cell Biol*. 1998; 109: 195–202.
7. **Torihashi S, Horisawa M, Watanabe Y.** c-Kit immunoreactive interstitial cells in the human gastrointestinal tract. *J Auton Nerv Syst*. 1999; 75: 38–50.
8. **Hagger R, Gharaie S, Finlayson C, *et al.*** Regional and transmural density of interstitial cells of Cajal in human colon and rectum. *Am J Physiol*. 1998; 275: G1309–16.
9. **Beckett EAH, Takeda Y, Yanase H, *et al.*** Synaptic specializations exist between enteric motor nerves and interstitial cells of Cajal in the murine stomach. *J Comp Neurol*. 2005; 493: 193–206.
10. **Huizinga JD, Thuneberg L, Kluppel M, *et al.*** W/kit gene required for interstitial cells of Cajal and for intestinal pacemaker activity. *Nature*. 1995; 373: 347–9.
11. **Ward SM, Burns AJ, Torihashi S, *et al.*** Mutation of the proto-onkogene c-kit blocks development of interstitial cells and electrical rhythmicity in murine intestine. *J Physiol*. 1994; 480: 91–7.
12. **Komuro T, Tokui K, Zhou DS.** Identification of the interstitial cells of Cajal. *Histol Histopathol*. 1996; 11: 769–86.
13. **Williams DE, Eisenmann J, Baird A.** Identification of a ligand for the c-kit proto-oncogene. *Cell*. 1990; 63: 167–74.
14. **Lecoin L, Gabella G, Le Douarin N.** Origin of the c-kit-positive interstitial cells in the avian bowel. *Development*. 1996; 122: 725–33.
15. **Torihashi S, Ward SM, Sanders KM.** Development of c-Kit-positive cells and the onset of electrical rhythmicity in murine small intestine. *Gastroenterology*. 1997; 112: 144–55.
16. **Young HM, Ciampoli D, Southwell BR, *et al.*** Origin of the interstitial cells of Cajal in the mouse intestine. *Dev Biol*. 1996; 180: 97–107.
17. **Kluppel M, Huizinga JD, Malysz J, *et al.*** Developmental origin and Kit-dependent development of the interstitial cells of Cajal in the mammalian small intestine. *Dev Dyn*. 1998; 211: 60–71.
18. **Beckett EAH, Ro S, Bayguinov Y, *et al.*** Kit signaling is essential for development and maintenance of interstitial cells of Cajal and electrical rhythmicity in the embryonic gastrointestinal tract. *Dev Dyn*. 2007; 236: 60–72.
19. **Sanders KM, Ordog T, Koh SD, *et al.*** Development and plasticity of interstitial cells of Cajal. *Neurogastroenterol Motil*. 1999; 11: 311–38.
20. **Gershon MD, Chalazonitis A, Rothman TP.** From neural crest to bowel: development of the enteric nervous system. *J Neurobiol*. 1993; 24: 199–214.
21. **Fu M, Chi Hang Lui V, Har Sham M, *et al.*** HOXB5 expression is spatially and temporarily regulated in human embryonic gut during neural crest cell colonization and differentiation of enteric neuroblasts. *Dev Dyn*. 2003; 228: 1–10.
22. **Fu M, Tam PK, Sham MH, *et al.*** Embryonic development of the ganglion plexuses and the concentric layer structure of human gut: a topographical study. *Anat Embryol*. 2004; 208: 33–41.
23. **Wallace AS, Burns AJ**. Development of the enteric nervous system, smooth muscle and interstitial cells of Cajal in the human gastrointestinal tract. *Cell Tissue Res*. 2005; 319: 367–82.
24. **Kenny SE, Connell G, Woodward MN, *et al.*** Ontogeny of interstitial cells of Cajal in the human intestine. *J Pediatr Surg*. 1999; 34: 1241–7.
25. **Wester T, Eriksson L, Olsson Y, *et al.*** Interstitial cells of Cajal in the human fetal small bowel as shown by c-kit immunohistochemistry. *Gut*. 1999; 44: 65–71.
26. **Faussone-Pellegrini MS, Vannucchi MG, Alaggio R, *et al.*** Morphology of the interstitial cells of Cajal of the human ileum from foetal to neonatal life. *J Cell Mol Med*. 2007; 11: 482–94.
27. **Komuro T.** Structure and organization of interstitial cells of Cajal in the gastrointestinal tract. *J Physiol*. 2006; 576: 653–8.
28. **Hanani M, Farrugia G, Komuro T.** Intercellular coupling of interstitial cells of Cajal in the digestive tract. *Int Rev Cytol*. 2005; 242: 249–82.
29. **Faussone-Pellegrini MS, Pantalone D, Cortesini C.** An ultrastructural study of the smooth muscle cells and nerve endings of the human stomach. *J Submicrosc Cytol Pathol*. 1989; 21: 421–37.
30. **Komuro T.** Comparative morphology of interstitial cells of Cajal: ultrastructural characterization. *Microsc Res Tech*.1999; 47: 267–85.
31. **Mitsui R, Komuro T.** Distribution and ultrastructure of interstitial cells of Cajal in the gastric antrum of wild-type and Ws/Ws rats. *Anat Embryol*. 2003; 206: 453–60.

32. **Horiguchi K, Semple GS, Sanders KM, *et al.*** Distribution of pacemaker function through the tunica muscularis of the canine gastric antrum. *J Physiol.* 2001; 537: 237–50.
33. **Mazet B, Raynier C.** Interstitial cells of Cajal in the guinea pig gastric antrum: distribution and regional density. *Cell Tissue Res.* 2004; 316: 23–34.
34. **Streutker CJ, Huizinga JD, Driman DK, *et al.*** Interstitial cells of Cajal in health and disease. Part I: Normal ICC structure and function with associated motility disorders. *Histopathology.* 2007; 50: 176–89.
35. **Cambrova P, Hubka P, Sulkova I, *et al.*** The pacemaker activity of interstitial cells of Cajal and gastric electrical activity. *Physiol Res.* 2003; 52: 275–84.
36. **Chen JD, Lin Z, Pan J.** Abnormal gastric myoelectrical activity and delayed gastric emptying in patients with symptoms suggestive of gastroparesis. *Dig Dis Sci.* 1996; 41: 1538–45.
37. **Lin X, Chen JZ.** Abnormal gastric slow waves in patients with functional dyspepsia assessed by multichannel electrogastrography. *Am J Physiol Gastrointest Liver Physiol.* 2001; 280: G1370–5.
38. **Ohshiro K, Yamataka A, Kobayashi Y.** Idiopathic gastric perforation in neonates and abnormal distribution of intestinal pacemakers cells. *J Pediatr Surg.* 2000; 35: 673–6.
39. **Rolle U, Piotrowska AP, Nemeth L, *et al.*** Altered distribution of interstitial cells of Cajal in Hirschsprung disease. *Arch Pathol Lab Med.* 2002; 126: 928–33.
40. **Yamataka A, Kato Y, Tibboel D, *et al.*** A lack of intestinal pacemaker (c-kit) in aganglionic bowel of patients with Hirschsprung's disease. *J Pediatr Surg.* 1995; 30: 441–4.
41. **Vanderwinden JM, Liu H, De Laet MH, *et al.*** Study of the interstitial cells of Cajal in infantile hypertrophic pyloric stenosis. *Gastroenterology.* 1996; 111: 279–88.
42. **Vanderwinden JM, Rumessen JJ.** Interstitial cells of Cajal in human gut and gastrointestinal disease. *Microsc Res Tech.* 1999; 47: 344–60.
43. **Min KW, Leabu M.** Interstitial cells of Cajal (ICC) and gastrointestinal stromal tumor (GIST): facts, speculations, and myths. *J Cell Mol Med.* 2006; 10: 995–1013.
44. **Torihashi S, Nishi K, Tokutomi Y, *et al.*** Blockade of kit signaling induces transdifferentiation of interstitial cells of Cajal to a smooth muscle phenotype. *Gastroenterology.* 1999; 117: 140–8.
45. **Thomsen L, Robinson TL, Lee JCF, *et al.*** Interstitial cells of Cajal generate rhythmic pacemaker current. *Nat Med.* 1998; 4: 848–51.
46. **Ward SM, Burns AJ, Torihashi S, *et al.*** Impaired development of interstitial cells and intestinal electrical rhythmicity in steel mutants. *Am J Physiol.* 1995; 269: C1577–85.
47. **Huizinga JD, Faussone-Pellegrini MS.** About the presence of interstitial cells of Cajal outside the musculature of the gastrointestinal tract, *J Cell Mol Med.* 2005; 9: 468–73.
48. **Harhun MI, Pucovsky V, Povstyan OV, *et al.*** Interstitial cells in the vasculature. *J Cell Mol Med.* 2005; 9: 232–43.
49. **Burns AJ, Lomax AE, Torihashi S, *et al.*** Interstitial cells of Cajal mediate inhibitory neurotransmission in the stomach. *Proc Nat Acad Sci USA.* 1996; 93: 12008–13.
50. **Song G, David G, Hirst S, *et al.*** Regional variation in ICC distribution, pacemaking activity and neural responses in the longitudinal muscle of the murine stomach. *J Physiol.* 2005; 564: 523–40.
51. **Suzuki H, Ward SM, Bayguinov YR, *et al.*** Involvement of intramuscular interstitial cells in nitrergic inhibition in the mouse gastric antrum. *J Physiol.* 2003; 546: 751–63.